VII. ELECTRON CYCLOTRON HEATING

M. PORKOLAB (MIT), P. T. BONOLI (MIT), R. C. ENGLADE (MIT), A. KRITZ (Hunter College), R. PRATER (GA), and G. R. SMITH (LLNL)

VII.A. INTRODUCTION

Electron cyclotron resonance heating (ECH) in BPX is planned as a possible upgrade to supplement the baseline ion cyclotron resonance frequency (ICRF) system. Eventual implementation primarily depends on the development of the required source technology. ECH offers important technical advantages over ICRF: High radio-frequency (RF) power density can be transmitted through ports ($P/A \gtrsim 100$ MW/m^2), and the antenna need not be in contact with the plasma for efficient coupling. In particular, low-field side, linearly polarized (O-mode) power injection will suffice. By controlling the $N_\parallel$ spectrum, or by steering the antenna, the power deposition profile can be controlled during ramping of the magnetic field even with a fixed frequency source. Because of the possibility of localized power deposition, ECH is a natural candidate for controlling magnetohydrodynamic (MHD) activity. Sawtooth oscillations may be prevented by heating in the vicinity of the $q = 1$ surface, and disruptions may be controlled by suppressing the $m = 2$ mode through localized heating near the $q = 2$ surface. In all cases of interest, ECH enjoys nearly 100% single-pass absorption in either D-T or pure hydrogen plasmas. Owing to the high densities in BPX, electron-ion temperature equilibration is very efficient, and there is little difference between direct electron or ion heating. Because of the remote antenna location, we expect that in the case of ECH, impurity generation associated with antenna-dependent RF sheath formation would be totally absent.

The main drawback of ECH at the present time is the lack of an available power source at the high frequencies of interest ($f \sim 250$ GHz). For this reason, ECH is not included in the BPX baseline, although the facility is designed to accommodate it. At present, source development is proceeding along two lines of approach, namely gyrotrons and free-electron lasers (FELs). It is expected that within this decade either approach may develop a $P \sim 1$ MW average RF power source at the desired frequency.

VII.B. NUMERICAL MODELING OF ECH-ASSISTED STARTUP

A simulation model for ECH has been developed[1] to accurately assess the feasibility of ECH-assisted startup and high-Q operation in BPX. This model is a combined code in which ECH ray tracing and absorption, an MHD equilibrium calculation, and thermal and particle transport are treated self-consistently. The ECH package is a variation of the TORAY code,[2] valid in the Doppler and relativistic regimes. Transport calculations are carried out using a modified version of the BALDUR $1\frac{1}{2}$-dimensional code.[3] Expressions for the electron and ion thermal diffusivity based on the "ITER89-P" empirical confinement scaling law[4] have been implemented in the transport package. It has been assumed that $\chi_e(r) \sim f(r)/\tau_E^{\rm ITER}$ and $\chi_i(r) = 2\chi_e(r)$, where $f(r)$ is an increasing function of plasma minor radius. In addition to providing a predictive tool for studying ECH in BPX, this simulation model will also be a valuable tool for analyzing the results of ECH experiments on DIII-D, TEXT, and MTX as they become available. As a result, we hope to determine an experimental $\chi(r)$ under ECH conditions that could then be used for predictive studies in BPX.

The heating scenarios studied for BPX thus far include ramping of the toroidal magnetic field, toroidal plasma current, and central electron density from 4.5 to 9 T, 1 to 11.8 MA, and 0.66 to 5.0×10^{20} m^{-3}, in 7.5 s. The ECH power is turned on from 4.5 to 7.5 s, and the angle of injection of the electron cyclotron rays is increased from 60 deg to 80 to 90 deg. The results of such a simulation are shown in Fig. 7.1. The effect of sweeping the angle of injection of the electron cyclotron waves is apparent in Fig. 7.1a where the ECH power deposition profile remains centralized as B_ϕ increased from 7.2 to 9 T during the period of ECH power injection. In this particular case, a parabolic density profile with $\tau_E^H = 2\tau_E^L$ was assumed, and a sawtooth period of $\tau_s = 0.3$ s was used. Similar cases have also been run with $\tau_s = 1.3$ s; however, the results are relatively insensitive to τ_s in the range of 0.3 to 1.3 s. The ECH power was launched from the low-field side of the torus at 252 GHz with $P_{EC} \simeq 20$ MW. In this case, $Q \approx 30$ was achieved during the RF pulse, where $Q = 5P_\alpha/(P_{aux}+P_{OH})$, neglecting dw/dt. Ignition

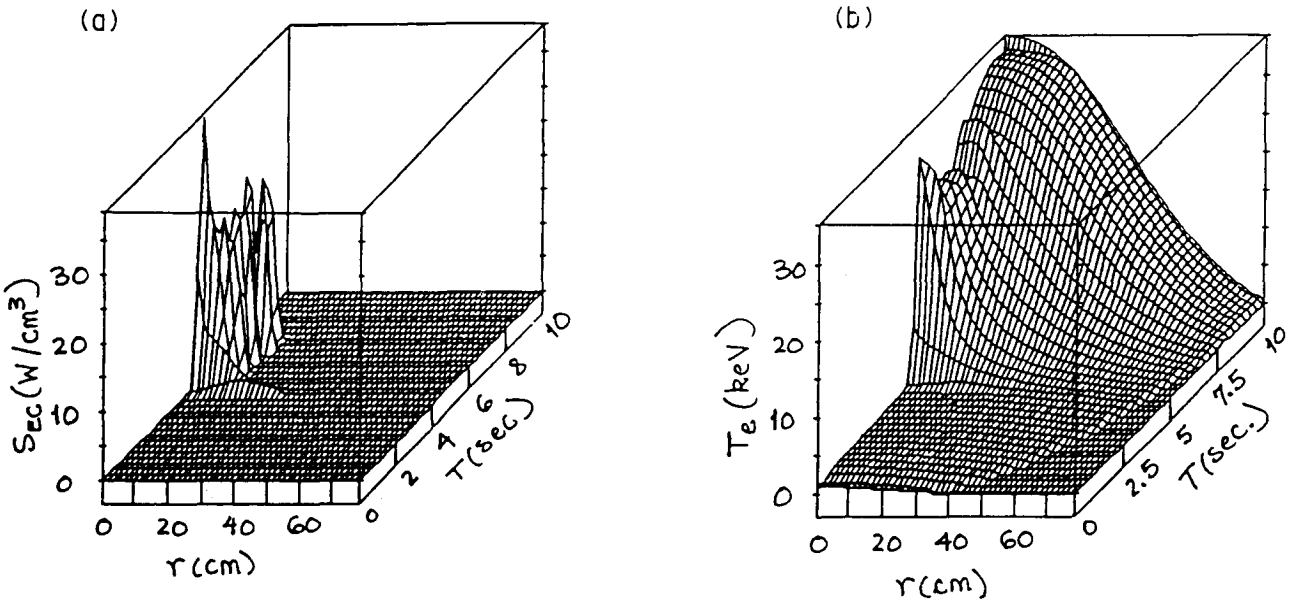

Fig. 7.1. ECH-assisted startup scenario in BPX using a parabolic density profile, $\tau_E^H = 2\tau_E^L$, and $P_{EC} = 20$ MW. The RF pulse is on from $t = 4.5$ s ($B = 7.2$ T) to $t = 7.5$ s ($B = 9$ T), and ignition occurs. (a) Temporal and spatial evolution of ECH power deposition profiles. (b) Temporal and spatial evolution of electron temperature.

occurs after the RF is turned off. If the density profile is changed to a square root parabolic, the value of Q decreases to 13 for these conditions. The use of an H-mode multiplier of less than 1.8 resulted in a 25 to 30% decrease in Q for both the parabolic and square root parabolic density profiles.

A potentially attractive ECH system would be one in which the RF beam is simply injected in the quasi-optical mode through the ports. Due to the long B_T ramp time (~20 s) we plan to heat only while the central magnetic field ramps from 8 to 9 T. Therefore, for perpendicular (or near-perpendicular) injection, the ECH resonance absorption layer moves from the high-field side ($r/a \simeq 0.4$) to the center as the magnetic field changes by $\delta B \sim 1$ T. We expect good single-pass absorption and effective heating with ECH even without steering the beam. Results for such a scenario are shown in Figs. 7.2a and 7.2b where we show ECH power deposition profiles at two values of the magnetic field. The temporal evolution of the temperatures and radial profiles are shown in Figs. 7.2c and 7.2d. These results show effective central heating of the plasma. Other parameters used in this example were a parabolic density profile, $\tau_E^H = 2\tau_E^L$, $n_e(0) = 5.5 \times 10^{20}$ m^{-3} (at flattop), $f_0 = 252$ GHz, and $P_{EC} = 20$ MW. In this case, $Q \approx 30$ was achieved with Q decreasing to about 13 to 15 for a square root parabolic density profile.

Recognizing the possibility of step-tunable frequency sources, we have considered the possibility of lower frequency operation at lower magnetic fields. In particular, a steady-state heating scenario in BPX was investigated recently, where ECH power was injected into a hydrogen discharge at 6 T and 7.9 MA. Machine operation at 2/3 field and current would result in a long-pulse capability for BPX (flattop period of about 45 s). Central ECH can be achieved at 6 T with a frequency of 224 GHz by injecting the electron cyclotron waves at a toroidal angle of 60 deg. An example of this is shown in Fig. 7.3, with $n_e(0) = 2 \times 10^{20}$ m^{-3}, $\tau_E^H = 1.85\tau_E^L$, $Z_{eff} = 2.0$, $P_{EC} = 30$ MW, no sawteeth, and a square root parabolic density profile. The ECH power is turned on from 3 to 6 s, and the deposition profile remains fairly centralized during the entire RF pulse (see Fig. 7.3a). The central electron temperature increases from 4 to 15 keV, and $T_i(0)$ increases from 4 to 10 keV (see Fig 7.3b).

It should be noted that the same frequency (224 GHz) may also be used in the 8 to 9 T ramp case if we wish to heat off-axis for the purposes of MHD control. However, 252 GHz cannot be used for central heating at 6-T field even at a 60-deg injection angle relative to the toroidal magnetic field. A lower frequency source may be required for central heating at 6 T, which may then be used for $m = 2$ MHD control (edge heating) at the full 9-T field operation. The lower frequency power would be beamed perpendicular to the toroidal field. This scenario will be studied in more detail as part of our future modeling studies.

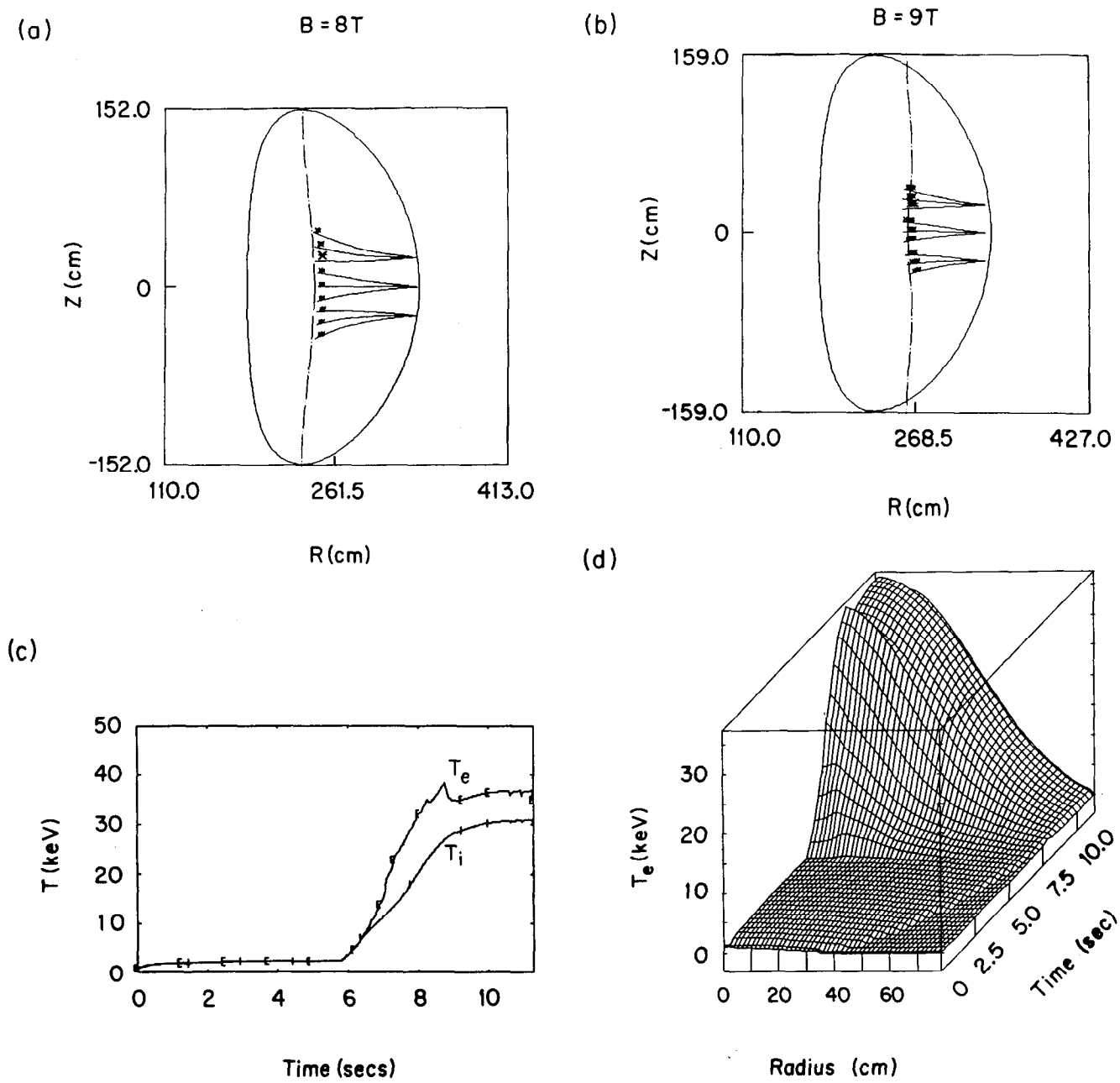

Fig. 7.2. ECH-assisted startup scenario in BPX using a parabolic density profile, $\tau_E^H = 2\tau_E^L$, and $P_{EC} =$ 20 MW. The RF pulse is on from $t = 5.75$ s ($B = 8$ T) to $t = 8.75$ s ($B = 9$ T), and ignition occurs. (a) Ray tracing and absorption (marked by the ticks on the rays) for three ray bundles launched in the poloidal plane. Each ray bundle consists of three rays with a spread of ±5 deg for a total power of 20 MW ($B = 8$ T). (b) Ray tracing and absorption (marked by ticks on the rays) for three ray bundles launched in the poloidal plane. Each ray bundle consists of three rays with a spread of ±5 deg for a total power of 20 MW ($B = 9$ T). (c) Temporal evolution of the central electron and ion temperatures. (d) Temporal and spatial evolution of the electron temperature profile.

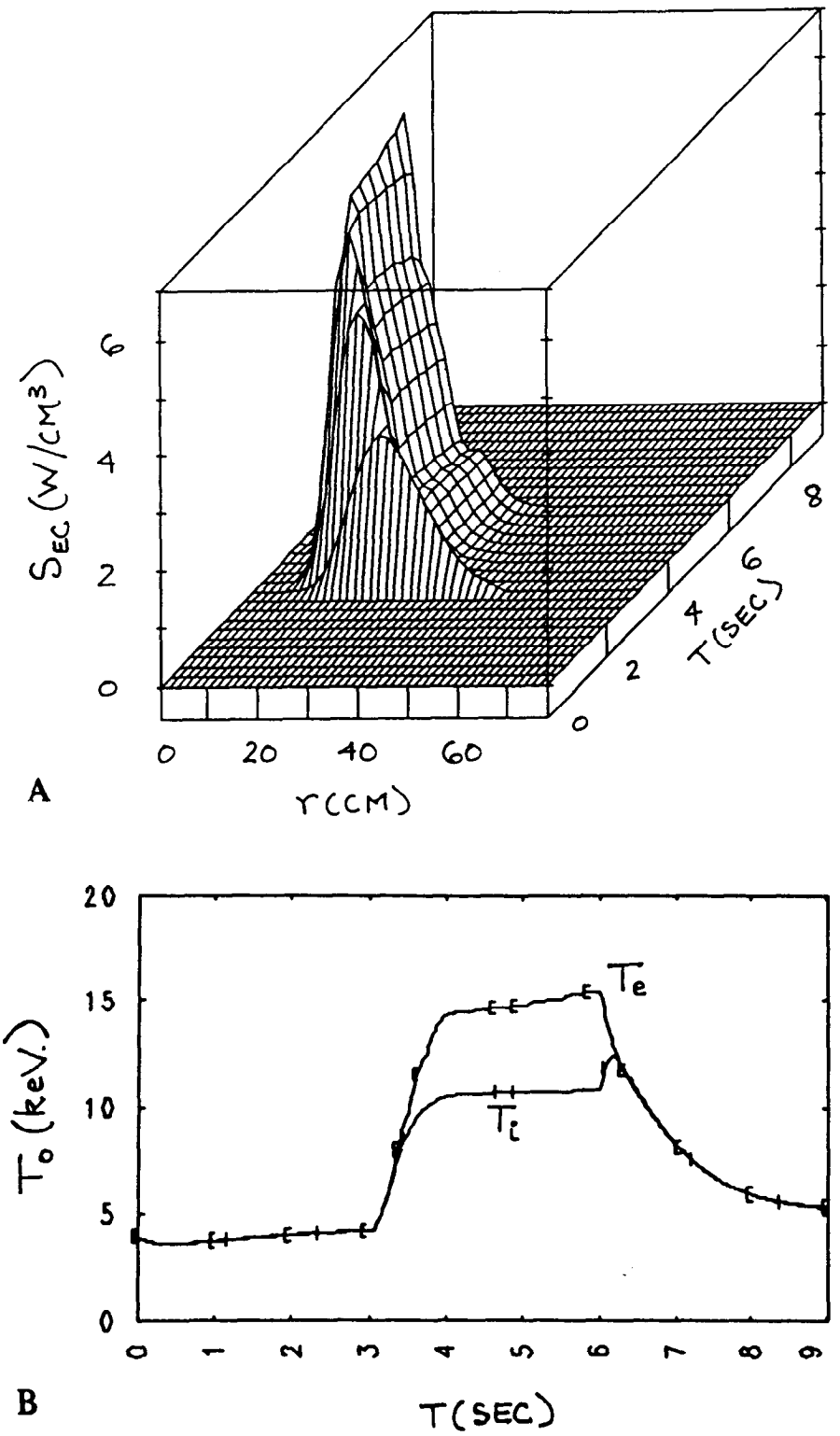

Fig. 7.3. ECH in a steady-state BPX scenario [$B_0 = 6$ T, $I_p = 7.9$ MA, $n_e(0) = 2 \times 10^{20}$ m^{-3}, $\tau_E^H = 1.85\tau_E^L$, $P_{EC} = 30$ MW, no sawteeth, and a square root parabolic density profile]. The RF pulse is on from 3.0 to 6.0 s. (a) Temporal and spatial evolution of the ECH power deposition. (b) Temporal evolution of the central electron and ion temperatures.

Another option is to use the 252 GHz sources for second-harmonic heating at 4.5 to 5 T long-pulse operation. The absorption efficiency at $\omega = 2\omega_{ce}$ for X-mode injection is comparable to that for O-mode at $\omega = \omega_c$. In particular, we obtain 100% single-pass absorption near the center even for perpendicular (or near-perpendicular) injection for X-mode at 4.5 to 5 T.

VII.C. MHD CONTROL STUDIES

In the area of MHD control, one of the key questions concerns localization of the RF power deposition profile. This depends on focusing the injected microwave beam, geometrical distribution of the incident microwave beam in the port, and possible scattering of the incident electron cyclotron rays by low-frequency fluctuations.

Very narrow profiles of ECH power deposition are thought to be necessary for control of the instabilities leading to sawtooth crashes and disruptions. These two instabilities require power deposition, respectively, near the $q = 1$ and $q = 2$ surfaces. For a nominal field of $B_0 = 9.0$ T, the cyclotron resonance frequencies at those surfaces are about 252 and 210 GHz. Injection of power along the equatorial plane, perpendicular to the magnetic field, at those frequencies can achieve deposition profiles with widths of approximately 1 cm at both $q = 1$ and $q = 2$. Given adequate power, such a two-frequency system should be able to control both instabilities.

Scattering by low-frequency drift-wave fluctuations does not significantly increase deposition profile widths for perpendicular injection.[5] This result follows from the very small $N_\parallel$ values typical of the fluctuations. The effect of scattering of the ECH beam is merely to increase the height of the beam cross section. The magnitude of the height increase is comparable to the diameter of a well-focused beam (about 10 cm) for turbulence levels consistent with mixing length estimates. Even with this increase, though, the beam height is very small compared with the total height of the plasma, and the scattering effects are therefore not significant.

A single-frequency system would be more desirable from a technological point of view than a two-frequency system, but initial studies indicate that localized power deposition near $q = 2$ is difficult with a frequency (252 GHz) appropriate for central heating or control of sawtooth crashes. Use of finite $N_\parallel$ to shift power deposition from the plasma center to the $q = 2$ surface results in a deposition profile that is much too wide for suppression of tearing-mode instabilities. If $N_\parallel$ is kept small, the power can be aimed within the poloidal plane so that the beam center intersects the $q = 2$ surface at the cyclotron resonance layer. Unfortunately, increased vertical divergence of the beam due to scattering by drift wave fluctuations is amplified by refraction effects and poor localization results (see Fig. 7.4).

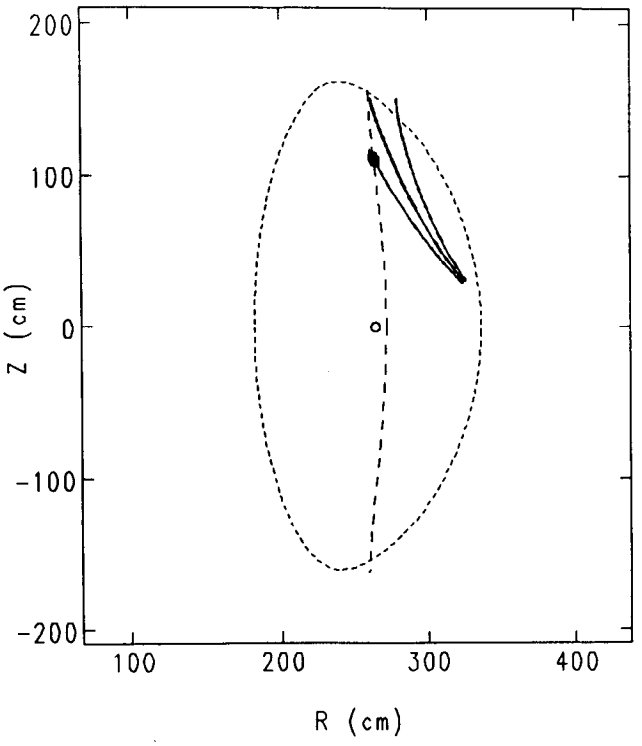

Fig. 7.4. Poor localizability of ECH power deposition with aiming in the poloidal plane. The launch angle θ_0 is measured between the ray and a horizontal plane. Parameters used were $B = 9$ T, $n_e(0) = 3 \times 10^{20}$ m^{-3}, $f_0 = 252$ GHz, and $\theta_0 = 50$ deg. The initial angular spread of the beam was chosen to model the effect of density fluctuation scattering.

The necessary power for stabilizing $m = 1$ or $m = 2$ modes, however, is not yet determined. There is some experimental evidence of sawtooth stabilization and $m = 2$ activity control using ECH on T-10, TFR, TEXT, and WT-3 (see Refs. 6 through 9). However, there is no general agreement on the interpretation of these results.[10] We are waiting for further experimental clarification from machines such as DIII-D on this important question. Theoretical investigations must also be continued on specifying power requirements.

Regarding the FEL sources, special questions arise in connection with the multi-GW peak power, which is delivered in short pulses. Initial stud-

ies indicate that, because of the relatively large ports in BPX (as compared with MTX), the importance of serious nonlinear effects is greatly reduced. In particular, neither filamentation- nor backscattering-type instabilities appears to be important when employing FEL sources in BPX (Ref. 11). Were it needed, the possible use of X-mode second-harmonic ECH (at ~500 GHz) with FEL sources would increase the cutoff density limit above $n_e \simeq 10^{21}$ m^{-3}.

VII.D. ECH ANTENNAS FOR BPX

The physics objectives of ECH in BPX can be accomplished by applying power at a fixed radial location, which implies rather simple antennas. Other possible objectives include control of sawteeth and stabilization of low-n modes for confinement improvement and disruption avoidance. These objectives require an antenna that can vary the location of the deposition on a rapid time scale. Such antennas are necessarily more complicated.

VII.D.1. Simple Antennas

The simplest ECH antenna is a conical horn that launches a narrow bundle of rays toward the plasma at a fixed angle. If the beam is narrow enough, the horn may be located far back in the port box, thereby taking advantage of the propagation of the ECH waves in free space without attenuation or loss of coupling efficiency. This arrangement has great advantages regarding thermal, mechanical, and maintenance properties of the antenna. For 252 GHz, the horn diameter may be 34 mm, which provides roughly a Gaussian beam with angular divergence of 2 deg (half-angle for 1/e in power). The power density of such a horn is 110 kW/cm^2, which is perfectly reasonable at that frequency. One horn per gyrotron would be required at the megawatt power level. This system is inherently broad-band, as it can accept a 30% change in frequency.

With this aperature (34 mm), the horns must be located approximately half-way from the flange to the plasma, about 1 m from the plasma. A support system for the end of the waveguide near the horn will be necessary to provide mechanical support and cooling. The mechanical support can probably be referenced only to the flange, thereby simplifying removal and replacement of the entire launcher system if remote maintenance is needed. The thermal load from the RF is low on the corrugated waveguide and horns, but some means of heat removal will probably be required. Pending a detailed design, it is anticipated that the mechanical support system can provide cooling through conduction to a water-cooled heat sink outside of the vacuum vessel.

An array of antennas can be installed in a single port. For a large radial port in BPX, for which the internal dimensions are 101 cm by 46 cm, an array of 4 wide by 8 high antennas should be feasible, for up to 32 MW in a single port if 1-MW gyrotrons are used. Even higher power on the port could be accomplished by reducing the diameter of the horns and packing the antennas more tightly.

VII.D.2. Steerable Antenna

To perform advanced applications of ECH such as sawtooth control or disruption control, it may be desirable to steer the ECH beam, as described in Ref. 2. This approach makes use of the Doppler shift to accomplish a radial shift in power deposition, by performing a rotation of the beam in the midplane relative to the radial. Angles between 0 and 30 deg from the radial should cover a wide range of applications. It should be noted that the angle that is needed depends on the magnetic geometry (e.g., location of the $q = 2$ surface) and the electron temperature profile, so that a sophisticated feedback system may be required to keep the power deposition in the required location.

This steering of the beam might be accomplished by placing a mirror assembly near the plasma end of the port box. One fixed mirror would be needed to direct the beam across the box in the toroidal direction, and another rotatable mirror would steer the beam toward the plasma. The same concept is used in the quasi-optical mode of transmission that is similar to that discussed in the System Design Document ECH section and in Ref. 2. This is probably a workable concept, although the mechanical and thermal design of the rotatable mirror is challenging. For long pulses at high power, it is likely that both mirrors would need to be actively cooled during the pulse. Mechanical linkages and bearings in the hostile reactor environment of BPX are very difficult to make, and magnetic forces due to disruptions will be difficult to manage.

An alternative scheme is to split the waveguide from each gyrotron into four to eight waveguides, each with fixed phase relative to the others. By controlling the phases of the multiple waveguides, which can be done from outside of the vacuum vessel, the beam can be steered in the toroidal direction. Each waveguide should be about 3 mm horizontally by perhaps 20 mm vertically, for an assembly dimension of 33 mm by 22 mm (assuming 1-mm walls). Packing of the antennas in a port box could probably be similar to that of the simple antennas described above, with similar requirements

on the support and cooling structures. One difference is that the antennas would have to extend closer to the plasma than simple antennas, due to the geometry of launching a wave at an angle from the radial. For 30 deg, the mouth of the phased array would have to lie less than 15 cm behind the first wall. This would increase the thermal load from the plasma. Windows, phase shifters, and diagnostics for beam properties would have to be developed, but viable concepts for these components exist.

VII.E. SUMMARY

To summarize, owing to its great potential, the capability to add ECH power is an important requirement for BPX. Advantages of ECH include localized heating, simple high-P/A launchers, and possibility of MHD control. The technological simplicity and lack of hardware close to the plasma are especially advantageous in a fusion environment.

REFERENCES

1. P. T. BONOLI, R. C. ENGLADE, M. PORKOLAB, and A. H. KRITZ, *Proc. 17th European Conf. Controlled Fusion and Plasma Heating,* Amsterdam, Netherlands, June 25–29, 1990, Vol. 14B, Part III, p. 1100, European Physical Society (1990).

2. R. C. MYER, M. PORKOLAB, G. R. SMITH, A. H. KRITZ, *Nucl. Fusion,* **29,** 2155 (1989).

3. G. BATEMAN, "Simulation of Transport in Tokamaks," *Computer Applications in Plasma Science and Engineering,* p. 381, A. T. DROBOT, Ed., Springer-Verlag, New York (1991).

4. K. BORRASS et al., "Summary Report for the June–October Joint Work Session, 1989 and Work Plan for 1990 ITER Project Unit Physics," ITER-ILPh-5-9-81.

5. G. R. SMITH, *Proc. 17th European Conf. Controlled Fusion and Plasma Heating,* Amsterdam, Netherlands, June 25–29, 1990, Vol. 14B, Part III, p. 1096, European Physical Society (1990).

6. V. V. ALIKAEV and K. A. RAZUMOVA, *Workshop on Applications of RF Waves to Tokamak Plasmas,* S. BERNABEI, U. GASPARINO, and E. SINDONI, Eds., EUR 10333 EN, Vol. I, p. 377 (1985).

7. TFR GROUP and FOM ECRH TEAM, *Nucl. Fusion,* **28,** 1995 (1988).

8. D. C. SING et al., *Bull. Am. Phys. Soc.,* **35,** 2026 (1990).

9. S. TANAKA, *Bull. Am. Phys. Soc.,* **35,** 2127 (1990).

10. R. PRATER, Private Communication.

11. M. PORKOLAB and B. COHEN, *Nucl. Fusion,* **28,** 239 (1988).